Synthesis, characterization, DNA binding of nano $Mn^{2+}$and Cu^{2+}complexes

Nashwa M. H Rizk[1], Samar A. Aly[1]*, Manal A. Khidr[1]

[1]*Department of Environmental Biotechnology, Genetic Engineering and Biotechnology Research Institute, University of Sadat City 32958, Egypt.*

DOI: 10.21608/RJAB.2022.292262

Corresponding author: Samar A. Aly
Tel: +201063936729
E-mail: samar.mostafa@gebri.usc.edu.eg

ABSTRACT

New complexes for Mn^{2+} and Cu^{2+} were prepared and characterized from ligand, 2-(phenylglycyl)-N-(p-tolyl)hydrazine-1-carbo thioamide (H2L) and binuclear Cu2+ complex (B3) of hydrazone derivatives . The structural compositions of the novel chelates were clarified using spectral, molar conductivity, FTIR, UV-Visible spectra,TGA, XRD and analytical techniques. The outcomes supported the ligand's neutral bidentate or monobasic tridentate behaviour. Coordination bonding has occurred via carbonyl oxygen (C=O) and N(2)H or (C-S) groups in complex (B1). The synthesized mononuclear complexes B1and B2 displayed an octahedral, square planar form. While B3 complex is binuclear. Also, the Cu^{2+}complex (B2) has a stronger antibacterial and anticancer activity than the Mn2+complex and the ligand when tested against different bacterial species and the HepG2 cell line. Respectively, the binding ability of ligand and Cu^{2+} complex (B2) with CT-DNA was aimed to for being intercalation or alternative strategy. The constant of intrinsic binding Kb was estimated.

Key words: Complexes, DNA binding, Infrared, TGA, Antibacterial.

1. INTRODUCTION

The bioactivities of hydrazine compounds and their metal complexes include alesprosy and mental disorder diseases treatment (Loncle *et al.,* 2003); antifungal (Singh *et al.,* 2008; Sharma *et al.,* 2009), antibacterial (Ibrahim *et al.,* 2009), anticonvulsant (Küçükgüzel *et al.,* 2003), anti-inflammatory (Melnyk *et al.,* 2006), analgesic (Lima *et al.,* 2000), antipla telets (Cunha *et al.,* 2003), anti-tuberculosis(Bedia *et al.,* 2006) and anticancer (Terzioglu and Gürsoy 2003) activities. It is believed that the synthesis of most stable chelates with transition metals that are already present inside the cell is what causes the tuberculostatic effect..As a result of , many significant enzymatic events catalysed by these transition metals are prevented by hydrazones (Cunha *et al.,* 2003).

Due to participation of several enzymes at redox changes, like superoxide dismutase, peroxidase, and dioxygenase, so that manganese chemistry is just a recent research focus (Lal *et al.,* 2006). Due to their outstanding magnetic characteristics and extensive biological diversity, manganese compounds are currently of great interest (Tasiopoulos *et al.,* 2004). In a crucial temperature, manganese-containing molecules can act as nanoscale magnetic particles or as nano magnets (Singh *et al.,* 2012). Moreover, due to stability and biocompatibility, copper complexes have the potential to be used in biological applications (Arjmand *et al.,* 2011). There has been a lot of focus on copper (II) complexes. coordination sphere flexibility enclosing $Cu^{2+}$and excess atoms allows for a variety of structural arrangements (Mugnai *et al.,* 2007).

Copper (II) feedback and offer models for metalloprotein activity and information for creating new catalysts (Patel *et al.*, 2020).

Complexes of Mn^{2+}, Fe^{2+}, Ni^{2+}, Co^{2+}, and Zn^{2+} and 2,6-diformyl--4-methylphenol di-benzoylhydrazone had synthesised and investigated utilising elemental analysis and spectro-scopic techniques(Cheng *et al.*,1995).The spectral, elemental, and Zn^{2+} chelates of 2--benzoylpyridinephenylhydrazone, 2-benzoyl pyrid-ine para- chloro phenyl hydrazine, and 2—benzoyl-pyridine para-nitrophenylhydrazone were studied using single crystal X-ray diffraction (Despaigne *et al.*, 2009).

Impact of gamma radiation on DNA interaction with Pd $^{2+}$, Cu^{2+}, and Cd^{2+} with 2-(phenylamino)-N-(thiophen-2-ylmethylene) aceto-hydrazide) (Aly *et al.*, 2021). Many studies have been conducted on metal hydrazone complexes with diverse functional groups (El-Tabl *et al.*, 2009). The creation, characterization , antimicrobial, and anticancer qualities of Manganese^{2+}and Copper^{2+} -complexes with 2-(phenylglycyl)-N-(p-tolyl) hydrazine-1-carbothioamide are the goals of this manuscript (H_2L).

2. MATERIAL AND METHODES

2.1. ligand synthesis (H_2L)

Necessary 2-(phenyl amino) aceto hydrazide (0.01 mol) was mixed with the appropriate amount of 1-isothiocyanato-4-methylbenzene (0.01 mol) in 10 ml of absolute ethanol to create the organic ligand 2-(phenyl glycyl)-N-(p-tolyl)hydrazine-1-carbothioamide (H_2L_B). For five hours, the combined reaction has been in reflux. Following cooling, the precipitate that resulted was filtered, washed by ethanol and three times, and vacuum dried with P_4O_{10} present (Abdalla *et al.*, 2021).

2.2. complexes Synthesis

Addition of a stoichiometric amount of MX_2, where M is Mn(II); Cu(II), and X is Cl in 100% ethanol to a heated ligand solution in (1L:1M)- molar ratio, metal complexes (B**1**-B_3) were created as indicated in Scheme 1.

At (60 ^oC), the resultant mixture was agitated using a magnetic field for (6-9 hrs). When still hot, the precipitate was removed,

Solution was preserved at 35 °C to allow part of the solvent to evaporate and aid in crystallisation. The crystals were extracted using vacuum filtrations, repeatedly cleaned with anhydrous diethylether, and then vacuum dried with P_4O_{10}.

2.3. Physical measurement

The ligand classification (H_2L) and their corresponding of $Mn^{2+}$and Cu^{2+} complexes was performed using a variety of spectroscopic methods (Section 1).

3. RESULTS and DISCUSSION

3.1 physical analysis

The quantitative and physical data about the 2-(anilinoacetyl)- N-(3-(methylpheny) hydrazine-1-carbothio amide ligand (H_2L) and its metal complexes were reported In table 1. Data indicate reactions between the ligand 2-(anilinoacetyl)- N-(3-(methylpheny) hydrazine-1-carbothio amide ligand (H_2L) and various Mn^{2+}, Cu^{2+}in 1M:1L produce mono metal complexes general formula, $[Mn(H_2L)_2Cl]$ and $[Cu(H_2L)\ Cl_2]$, while reactions with complex (B_3) produce binuclear complexes of general formula$[Cu_2(H_2L)(OH)_2(H_2O)_2\ Cl.Cl.2H_2O]$. Mn^{2+} and Cu^{2+} complexes are non-electrolytes, based on the molar conductivities in the DMF - solution (Table 1) (Abdalla *et al.*, 2020; Bayoumi *et al.*, 2013).

3.2 FT-IR spectra

3.2.1. IR- spectra of ligand

Comparison of the ligand's functional groups (H_2L) in the case of using infrared spectra Table 2 and Figure 1 in which; the stretching frequencies of (N4-H), (N2-H),

and (N1-H), as well as (C=O) and (C=S) correspondingly, have been discovered to be responsible for the the ligand functional groups ; that exhibit at 3384, 3263, 3150, 1672, 1689, and 749 cm^{-1}.

3.2.2. IR- Spectra of Mn (II) complex

IR- spectra of Mn(II) complexes Fig. 1 (a,b) show strong bands at 3428, 3272, 3014, 1668, 750 cm^{-1} which linked assigned to the wagging vibrations of (N4-H), (N2-H), (N1-H), (C=O), and (C=S) stretching frequencies, respectively .The IR spectra of complexes it is seen that the band corresponding to υ(N2-H) and υ(C=O) shift to higher and lower frequency as compared of free. The new bands, which were ascribed to the elements Mn-O and Mn-N, respectively, appear at 637 and 505 cm^{-1} (Aly and Elembaby, 2020).

3.2.3. IR Spectra of Cu(II) complexes

Cu (II) complex (B_2) exhibited sharp and strong bands at (3300, 3210, 3150), (1645, 735 cm^{-1} while the (B3) complex revealed bands at 3435, 2921, 1620, and 1540 cm-1 assigned to (O-H); (N1-H); (C=O) and (C=N) accordingly. These bands were explained by the stretching frequencies of (N4-H), (N2-H), (N1-H), (C=O), and (C=S). New bands of υ-(M-O) and υ(M-N) appeared at (480, 550) and (430, 485) cm^{-1} wagging vibrations in (B2 and B3) , respectively. These bands move to lower frequency as compared to single ligand and the coordination via (N1-H), (C=O) groups in (B_2) complex , υ(C=O) and υ(C=N) in (B_3) complex and the ligand behaves as neutral bidentate.

3.3. UV-Visible spectra and magnetic moment

The approach was used for evaluating the electronic absorption ligand spectra, Mn (II), and Cu (II) complexes (B_1-B_3) appear at the region among 200-800 nm, as shown in table 3 and Fig. 2. Some shifts can be seen in the electronic spectra of free ligands and their metal complexes, which can be regarded as confirmation of complex formation. Bands at 279 and 292 nm, respectively, are visible in the ligand's electronic spectrum and can be attributed to π -π* transitions.

3.3.1. Mn (II) Complex

The weak absorption bands at 28169.01 and 22675.74 cm^{-1} in each combination can be attributed to the transitions 6A1g→ 4E1g and 4A1g (4G) in the Mn (II) complex absorption spectra shown in Fig. 2. The measured magnetic moments of 5.81 BM confirm the octahedral shape for the Mn (II), with five unpaired electrons in the complex, in accordance with the d^5-electronic configuration of Mn (II), where an effective magnetic moment for slightly high spin complexes is estimated to be (6.0) BM (Refat and El-Metwaly 2012).

3.3.2 Cu (II) Complex

Three peaks were found at 32050, 30120, and 26890 cm^{-1} that can be attributed at n-π* and CT transitions are visible in the electronic band of absorption spectra of the Cu (II) complex (B_2) as well as a d-d band at 15700 Cm^{-1}. The highest energy 2B1g→2A1g transition, which has a square planar shape, dominates the Cu (II) complex's visible electronic absorption spectrum. While the Cu (II) complex (B_3) produces a binuclear complex, absorption bands corresponding for the n-π* and CT transitions, as well as the d-d band, emerge at cm-1 values of 32058, 26885, 15700, and 15800. The magnetic susceptibility value is 1.68, 3.4B.M., which points to a square environment surrounding the Cu (II) ion(B_2) (Konstantinovic *et al.*, 2003) and binuclear complex of (B_3).

3.4. Thermal studies (TGA)

Thermogravimetric procedures were used to Examine the ligand, Mn (II), and Cu (II) complexes' temperature behaviour. in the temperature range of 25-800 °C. The ligand's TG curve (Fig. 3) demonstrates

that it is thermally stable up- to 125 °C; and undergoes total breakdown at 565 °C.

3.4.1. Mn (II) and Cu (II) Complex

Complexes (B_1-B3) have three steps in their TGA curves (Figs. 4, 5, 6), with the first step showing weight loss at 114-195, 180-225, and 37-126 ºC (Calc./Find%: 29.89/29.90, 5.8/5.6, and 5.58/6.0), which agrees with the loss of the $C_8H_8N_3S$ moiety plus one molecule of hydrogen chloride and two hydrated water. The second step, which corresponds to the dissociation of $C_{16}H_{17}N_4OS$, HCl+0.5 of ligand, two coordinated waters, and ionized chloride, is carried out in the temperature ranges of 195–331 and 225–610°C with mass loss (Calc./ Found%: 43.63–43.65, 43.1/43.0, and 12.08–11.33). The third stage has been identified as the removal of C8H9NO, total decomposition of organic components, and $C_{14}H_{16}NS$ with weight loss (Calc./Found%: 18.82 /18.75, 34.8 /34.6, and 42.92/42.63), leaving final residues of manganese, copper metal, and two coppers.

3.5. XRD pattern

Copper chelates (B3) powder XRD patterns Fig.7 was displayed. Using (Cu K) radiation (1.5406), the X-ray diffraction was observed. The scanning field of view was 5-80 nm. XRD patterns of powder particles that are a copper complex (amorphous).

3.6. Biological application

3.6.1 DNA binding and Cu (II) complex

To assess a metal complex's capacity to attach to a DNA- helix, electronic absorption - spectroscopy is frequently used (Li *et al.,* 2017).Complexes joined to DNA through intercalation commonly show lowering in molar absorptivity (hypo-chromism) and a redshift (batho-chromism) of their electronic absorption bands because of the strong stacking contact between the complex's aromatic chromo-phores and DNA base-pairs (Long and Barton 1990). The copper complex (B_2) and ligand (H_2L) demonstrated that, the absorption intensity-ies gradually declined with increasing the concentration of DNA (0, 0.2, 0.4, 0.6, 0.8, and 1 Mm), i.e., a considerable hyperchromic impact was noticed upon the addition of more quantities of CT-DNA. As opposed to the traditional intercalation binding, this revealed the presence of strong contact between the ligand (H_2L) and copper complex (B_2) with CT-DNA. It is discovered that the intercalative binding strength correlates with the degree of shift and hypochromism (Eswaran *et al.,* 2019). Figures depict the copper complex (B_2) and ligand (H_2L) absorption spectra in the presence and absence of herring sperm DNA (8, 9). The alterations that were seen after gradually adding DNA to test compounds demonstrate that the ligand and copper complex was tightly attached to DNA via the intercalative mechanism. The ligand (H_2L) absorption bands had a hyperchromism of about 18.4% at 400 nm in the presence of DNA. Nevertheless, copper complex (B_2) displayed hyperchromism of approximately 30.5% at 320 nm for (B2), together with bathochromic shifts of 2 nm for (B_2), which demonstrate that the ligand and copper complex were tightly attached to DNA via the mode of intercalation. According to stacking interactions between DNA- base pairs and aromatic chromo-phores of the complexes, which is consistent with the intercala-tive mechanism of binding, Hyperchromism was found [Saini *et al.,* 2015; Griffin *et al.,* 2013). These findings are comparable to those that have previously been reported for different metallo- intercalators (Sirajuddin *et al.,* 2013).

for comparing quantitatively the binding strength of the compounds, the intrinsic binding-constants (K_b) of them with CT-DNA were estimated by this equation (1) (Aly *et al.,* 2021; El-Tabl *et al.,* 2009).

$$[DNA]/(\varepsilon_a - \varepsilon_f) = [DNA]/(\varepsilon_b - \varepsilon_f) + 1/[K_b(\varepsilon_b - \varepsilon_f)] \quad \ldots(1)$$

K_b was estimated by the slop ratio to intercept, that were reported to be 1.2 x 10^6 M^{-1} for (H_2L), 1.9 x 10^6 M^{-1} for (B_2) respectively. The magnitude value of binding constant clearly showed that cobalt complex (B_2) bound most strongly with DNA than the ligand through an intercalation mode. It should be noticed complex geometry that affects the magnitude of binding.

3.6.2. Anti-bacterial activity

The antibacterial action of the ligand and its complexes of Mn(II), Cu(II), Ag(I), and Cd(II) were tested against the bacterial species, including Streptococcus pyogenes and Escherichia coli. Table 5 and Figs. 10 and 11 show how efficient the ligand and copper complex's antibacterial action are. These findings show that complexes are more active than ligand and (Abdalla *et al.*, 2020; Aly and Elembaby 2020). The complexes highest activity can be demonesterated on basic of Overtone's-concept (Anjaneyulu and Rao 1986) as shown in many of our previous investigations (Hassan *et al.*, 2020; Hassan and Khalf-Alla 2020; Khalf-Alla *et al.*, 2019). During chelation, metal ion's polarity can be decreased due to the involvement of its partial positive charge with donation sites of the coordinated ligand. Moreover, chelation makes it easier for π-electrons to delocalize throughout the entire chelate ring, which improves the studied compound's lipophilic properties. Because of its lipophilic nature, the chemical can more easily pass through the lipid layer of cell membranes, which causes more aggressive cell death. The Cu (II) complex (B_2) also gains stronger antibacterial activity and moves in the following order: B2 > B1 > > H_2L.

3.6.3 Cytoxicity

Exhibition of cytotoxic effects of the ligand and their complexes against human liver cancer cell line ($HepG_2$) before and after irradiations Table 6 and Figure 12. The results are being expressed as IC_{50}, which is the medication concentration that, when compared with the control cells growth, results in (50%) reduction in the proliferation of cancer cells. It was discovered that the Cu (II) complex and thiosemicarbazide ligand were more physiologically active than the Mn (II) complex. Moreover, the Mn (II) complex and ligand are lower than the Cu (II) complex., where the IC_{50} value are following order:

Vinblastine (4.58) > B_2 (23.21) > B_1 (28.23) > H_2L (31.26) µg/mL

4. CONCLUSION

New Mn(II), Cu(II) complexes were created and characterized. Summarized results are the following:

1- Mn(II) complex is octahedral, while Cu(II) complex is square planner geometry and Cu(II) complex- (B_3) is binuclear complex .
2- The CT-DNA binding affinity of the ligand and Cu(II) complex were estimated, and the intrinsic binding constant K_b was quantified and arranged asthe following: B_2 (1.9 × 10^6) > H_2L (1.2 × 10^6) mol^{-1} dm^{-3}.
3- The Cu complexes have higher activity than ligand and Mn complex (B1) acquires better antibact-erial activity.
4- The created ligand, and its complexes act as a well anticancer effect on the $HepG_2$ cell line before irradiation, and Cu(II) complexes are most higher than of them. Moreover, vinblastine has an enhanced anticancer effect on the targeted cancer cell lines.

5. REFERENCES

Abdalla, E.M., Hassan, S.S., Elganzory, H.H., Aly, S.A., Alshater, H., (2021). Molecular Docking, DFT Calculations, Effect of A.A.High Energetic Ionizing Radiation, and Biological Evaluation of Some Novel

Metal (II) Heteroleptic Complexes Bearing the Thiosemicarbazone Ligand. Molecules, **26**(19), 5851.

Abdalla, E.M., Abdel Rahman, L.H., Abdelhamid, A.A., Shehata, M.R., Alothman, A.A., Nafady, A., (2020). Synthesis, Characterization, Theoretical Studies, and Antimicrobial/Antitumor Potencies of Salen and Salen/Imidazole Complexes of Co (II), Ni (II), Cu (II), Cd (II), Al (III) and La (III), Appl. Organomet. Chem, **34**(11), e5912.

Aly, S. Elembaby, S., (2020). Synthesis, spectroscopic characterization and Study the effect of gamma irradiation on VO2+, Mn2+, Zn2+, Ru3+, Pd2+, Ag+ and Hg2+ complexes and antibacterial activities. Arabian Journal of Chemistry ,**13**(2), 4425-4447.

Aly, S.A., Elganzory, H.H., Mahross, M.H., Abdalla, E.M., (2021). Quantum chemical studies and effect of gamma irradiation on the spectral, thermal, X-ray diffraction and DNA interaction with Pd (II), Cu (I), and Cd (II) of hydrazone derivatives. Applied Organometallic Chemistry, **35**(4), e6153.

Anjaneyulu, Y., Rao, R.P., (1986). Preparation, characterization and antimicrobial activity studies on some ternary complexes of Cu (II) with acetylacetone and various salicylic acids.Synthesis and Reactivity in Inorganic and Metal-Organic Chemistry,**16**(2) , 257-272.

Arjmand, F., Sayeed, F., Muddassir, M., (2011). Synthesis of new chiral heterocyclic Schiff base modulated Cu (II)/Zn (II) complexes: their comparative binding studies with CT-DNA, mononucleotides and cleavage activity. Journal of Photochemistry and Photobiology B. Biology,**103**(2):166-179.

Bayoumi, H.A., Alagha A., Aljahdali, M.S., (2013). Cu (II), Ni (II), Co (II) and Cr (III) complexes with N2O2-chelating schiff's base ligand incorporating azo and sulfonamide moieties: spectroscopic, electrochemical behavior and thermal decomposition studies. Int. J. Electrochem, Sci, **8**, 9399-9413.

Bedia, K., Elçin, O. Seda, U., Fatma, K., Nathaly, S., Sevim, R., Dimoglo, A., (2006). Synthesis and characterization of novel hydrazide–hydrazones and the study of their structure–antituberculosis activity. European journal of medicinal chemistry, **41**(11), 1253-1261.

Cheng, P., Liao, D., Yan, S., Jiang, Z., Wang, G., (1995). Synthesis and characterization of some binuclear transition metal complexes of a binucleating ligand. Polyhedron, **14**, 2355-2359.

Cunha, A., Figueiredo, J., Tributino, J., Miranda, A., Castro, H., Zingali, R., Fraga, C., de Souza, AM., Ferreira, MCBV., Barreiro, VF., (2003). EJ, Bioorg. Med. Chem, **11** ,2051.

Mugnai, M., Cardini, G., Schettino, V., Nielsen, C.J., (2007). Ab initio molecular dynamics study of aqueous formaldehyde and methanediol. Molecular Physics; **105**,2203-2210.

Despaigne, A.A.R., Da Silva, J.G., do Carmo, A.C.M., Piro, O.E., Castellano, E.E., Beraldo, H. (2009). Structural studies on zinc (II) complexes with 2-benzoylpyridine-derived hydrazones. Inorganica Chimica Acta, **362**,2117-2122.

El-Tabl, A.S., El-Bahnasawy, R.M., Hamdy, A.E.-D., (2009). Synthesis, magnetic, spectral and antimicrobial studies on metal complexes of 4-methylphenylaminoacetoisatin hydrazone., Journal of Chemical Research, **2009**, 659-664.

Eswaran, J., Sankar, N.K., Bhuvanesh, N.S., Velusamy, K.M., (2019). Ruthenium hydrazone complexes with 1: 1 and 1: 2 metal–ligand stoichiometry: a comparison of biomolecular interactions and in vitro cytotoxicities. Transition Metal Chemistry, **44**(4),369-382.

Griffin, M.D., Ryan, A.E., Alagesan, S. Lohan, P., Treacy, O., Ritter, T., (2013). Anti-donor immune responses elicited by allogeneic mesenchymal stem cells: what have we learned so far? Immunology and cell biology, **91**(1), 40-51.

Hassan, S.S., Shallan, R.N, Salama, M.M., (2020). Antibacterial and molecular study of thiourea derivative ligand and its Dimethyltin (IV) complex with the superior of its Copper (II) complex as a hepatocellular antitumor drug.J. Organomet. Chem, **911**, 121115.

Hassan, S.S., Khalf-Alla, P.A., (2020). Anti-hepatocellular carcinoma, antioxidant, anti-inflammation and antimicrobial investigation of some novel first and second transition metal complexes. Appl. Organomet. Chem, 34(4), e5432.

Ibrahim, K., Gabr, I., Abu El-Reash, G., Zaky, R., (2009). Spectral, magnetic, thermal, antimicrobial, and eukaryotic DNA studies on acetone [N-(3-hydroxy-2-naphthoyl)] hydrazone complexes. Monatshefte für Chemie-Chemical Monthly, **140(6**), 625-632.

Khalf-Alla, P.A., Hassan, S.S., Shoukry, M.M., (2019). Complex formation equilibria, DFT, docking, antioxidant and antimicrobial studies of iron (III) complexes involving Schiff bases derived from glucosamine or ethanolamine. Inorganica Chim. Acta,**492**,192-197.

Konstantinovic, S.S., Radovanović, B., Cakic, Z., Vasić, V.M., (2003). Synthesis and characterization of Co (II), Ni (II), Cu (II) and Zn (II) complexes with 3-salicylidenehydrazono-2-indolinone. Journal of the Serbian Chemical Society, **68**, 641-647.

Küçükgüzel, S.G., Mazi, A., Sahin, F. , Öztürk, S., Stables, J. , (2003). Synthesis and biological activities of diflunisal hydrazide–hydrazones. European journal of medicinal chemistry; **38**, 1005-1013.

Lal, R.A., Bhaumik, S., Lemtur, A., Singh, M.K., Basumatari, D., Choudhury, S., De, A., Kumar, A., (2006). Synthesis, characterization and crystal structure of manganese (IV) complex derived from salicylic acid. Inorganica chimica acta, **359**(10), 3105-3110.

Li, Y., Yang, Z., Zhou, M., Y. Li, Y., He, J., Wang, X., Lin, Z., (2017). Ni (II) and Co (II) complexes of an asymmetrical aroylhydrazone: synthesis, molecular structures, DNA binding, protein interaction, radical scavenging and cytotoxic activity. RSC advances ,**7**, 41527-41539.

Lima, P., Lima, L., Da Silva, K., Léda, P. , Miranda, A., Fraga, LP, (2000). CAM; Barreiro, EJ, Eur. J. Med. Chem, **35**, 187.

Loncle, C., Brunel, J.M., Vidal, N., Dherbomez, M., Y. Letourneux, Y., (2004). Synthesis and antifungal activity of cholesterol-hydrazone derivatives. European Journal of Medicinal Chemistry, **39**(12), 1067-1071.

Melnyk, P. , Leroux, V., Sergheraert, C. , Grellier, P., (2006): Design, synthesis and in vitro antimalarial activity of an acylhydrazone library, Bioorganic & medicinal chemistry letters **16(1)**, 31-35.

Patel, A.K., Jadeja, R.N., Roy, H., Patel, R., Patel, S.K., Butcher, R.J., Cortijo, M., Herrero, S. (2020). Copper (II) hydrazone complexes with different nuclearities and geometries: Synthesis, structural characterization, antioxidant SOD activity and antiproliferative properties. Polyhedron,**186** ,114624.

Refat, M.S, El-Metwaly, N.M., (2012). Spectral, thermal and biological studies of Mn (II) and Cu (II) complexes with two thiosemicarbazide derivatives. Spectrochimica Acta Part A: Molecular and Biomolecular Spectroscopy, **92**, 336-346

Saini, R.K., Nile, S.H., Park, S.W., (2015). Carotenoids from fruits and

vegetables: Chemistry, analysis, occurrence, bioavailability and biological activities. Food Research International,**76**, 735-750.

Sharma, K., Sharma, V., Dubey, R., Tripathi, U., (2009). Antimicrobial and anti-inflammatory studies of 5 (2′-hydroxyphenyl)-3-(4-x-phenyl) pyrazolinates of copper (II) and their addition complexes with donor ligands. J Coord Chem, **62(3)**, 493.

Singh, M., Bharty, M.K., Singh, A., Kashyap, S., Singh, U.P., Singh, N.K., (2012). Mn (II) complexes of N′-(2-methoxybenzoyl) hydrazine carbodithioic acid ethyl ester: synthesis, spectral and structural characterization. Transition Metal Chemistry, **37**(8) ,695-703.

Singh, V.P., Katiyar, A., Singh, S., Synthesis, (2008). characterization of some transition metal (II) complexes of acetone p-amino acetophenone salicyloyl hydrazone and their antimicrobial activity. Biometals, **21(4**), 491-501.

Sirajuddin, M., Ali, S., Badshah, A. (2013). Biology Drug—DNA interactions and their study by UV—Visible, fluorescence spectroscopies and cyclic voltametry.J. Photochem. Photobiol. B Biol, **124**, 1-19.

Tasiopoulos, A.J., Wernsdorfer, W., Abboud, K.A., Christou, G., (2004). A Reductive-Aggregation Route to [$Mn_{12}O_{12}$ (OMe) 2 (O_2CPh) 16 (H_2O) $_2$] 2− Single-Molecule Magnets Related to the [Mn12] Family. Angewandte Chemie, **116**(46): 6498-6502.

Terzioglu, N., Gürsoy, A., (2003). Synthesis and anticancer evaluation of some new hydrazone derivatives of 2, 6-dimethylimidazo [2, 1-b][1, 3, 4] thiadiazole-5-carbohydrazide. European journal of medicinal chemistry, **38**,781-786.

Table (1): Elemental analyses and physical properties of ligand (H_2L) and Mn(II), Cu(II) complexes.

No.	Compounds	Color Yield %	Mol. Wt	Found (Calc.) %					Am
				C	H	N	Cl	M	
H_2L	$C_{16}H_{18}N_4OS$	Buff 75	314.41	61.12(61.09)	5.77(5.74)	17.82(17.78)	—	—	—
B_1	$C_{32}H_{35}N_8O_2S_2ClMn$	Brown 70	718.19	53.49(53.52)	4.87(4.91)	15.54(15.60)	4.91(4.94)	7.59(7.65)	25
B_2	$C_{16}H_{18}N_4OS\ Cl_2Cu$	Dark green 85	448.85	42.4(42.81)	4.1(4.04)	12.26(12.48)	15.91(15.80)	14.11(14.16)	23
B_3	$C_{15}H_{27}N_3O_6S\ Cl_2Cu_2$	Brown 75	591	30.6(30.46)	4.2(4.57)	7.3(7.10)	12.31(12.00)	21.70(21.50)	80

Where: Λm=molar conductivity (ohm-1 cm2 mol-1) in 10^{-3} M DMF soluti

Table (2): Infrared spectral bands (cm-1) for ligand, Mn(II) and Cu(II) complexes

No	Compound	ν (OH)/(N4-H)	ν(N2-H)	ν(N1-H)	ν(C=O)	ν(C=S)	ν(M-O)	ν(M-N)
H_2L	$C_{16}H_{18}N_4OS$	3384	3263	3150	1672	749	—	—
B_1	$C_{32}H_{35}N_8O_2S_2ClMn$	3428	3272	3014	1668	750	637	505
B_2	$C_{16}H_{18}N_4OSCl_2Cu$	3300	3210	3150	1645	735	480	430
B_3	$C_{15}H_{27}N_3O_6S\ Cl_2Cu_2$	3435	-	-	1620	-	550	485

Table (3) : The magnetic moment values and electronic absorption spectral data in DMF solution of ligand and Mn(II) and Cu(II) complexes .

No	*Compounds*	*λmax (DMF)*	μ_{eff} *(B.M.)*
		(cm^{-1})	
H_2L	*$C_{16}H_{18}N_4OS$*	*35842.29, 34246.58*	—
B_1	*$C_{32}H_{35}ClMnN_8O_2S_2$*	*28169.01, 22675.74*	*5.81*
B_2	*$C_{16}H_{18}Cl_2CuN_4OS$*	*32050, 30120, 26890, 15700*	*1.68*
B_3	*$C_{15}H_{27}N_3O_6S\ Cl_2Cu_2$*	*32058, 26885, 15700, 15800*	*3.4*

Table 4: Thermal analysis data of ligand and Mn (II), Cu (II)complexes

No.	Compound	Temp. range (°C)	Mass loss% Calc.(F)		Assignment
H_2L	$C_{16}H_{18}N_4OS$	125-201	33.76	(33.72)	C_7H_8N
		201-435	49.35	(49.38)	$C_5H_5N_3OS$
		435-565	16.88	(16.90)	C_4H_5
B_1	$C_{32}H_{35}ClMnN_8O_2S_2$	114-195	29.89	(29.90)	$C_8H_8N_3S$+HCl
		195-331	43.63	(43.65)	$C_{16}H_{17}N_4OS$
		331-515	18.82	(18.75)	C_8H_9NO
	Residue	> 515	7.65	(7.64)	Mn
B_2	$C_{16}H_{18}Cl_2CuN_4OS$	180-225	5.8	(5.9)	C_2H_2
		225-610	43.1	(43.0)	HCl+0.5L
		610-800	34.8	(34.6)	Complete decomp.
	Residue	At 800	14.1	(14.2)	Cu
B_3	$C_{15}H_{27}N_3O_6S\ Cl_2Cu_2$	37-126	5.58	(6.0)	Hydrated
		126-232	12.08	(11.33)	2 coordinated water
		232-398	42.92	(42.63)	+ ionized chloride
		398-600	11.50	(10.99)	$C_{14}H_{16}NS$
	Residue	**Above 600**	29.60	(29.08)	Remaining 2Cu+4C

Table 5: Antibacterial activity of ligand and their metal complexes

No.	Compound	Inhibition %					
		S. pyogenes			***E.coli***		
		1µg/ml	**5µg/ml**	**10µg/ml**	**1µg/ml**	**5µg/ml**	**10µg/ml**
H_2L	**$C_{16}H_{18}N_4OS$**	75.32	90	94.1	48.76	56.23	61.2
B_1	**Mn (H_2L) (HL)**	76.09	91.32	96.91	59.52	92.81	96.62
B_2	**Cu (H_2L)Cl_2**	80.34	94.82	99.81	70.63	95.00	98.21
B_3	**Cu_2 (H_2L) $(OH)_2$ $(H_2O)_2Cl$**	80.34	94.82	99.81	70.64	95.0	98.21

Table. 6. Cytotoxic activity (IC_{50}) of the ligand and some metal complexes againsthuman liver $HepG_2$ cancer.

No	*Compound*	*IC50 (µM)*
H_2L	$C_{16}H_{18}N_4OS$	*31.26*
B_1	$C_{32}H_{35}ClMnN_8O_2S$	*28.23*
B_2	$C_{16}H_{18}Cl_2CuN_4OS$	*23*
B_3	$C_{15}H_{27}N_3O_6S\ Cl_2Cu_2$	*23*
Vinblastine		*4.5*

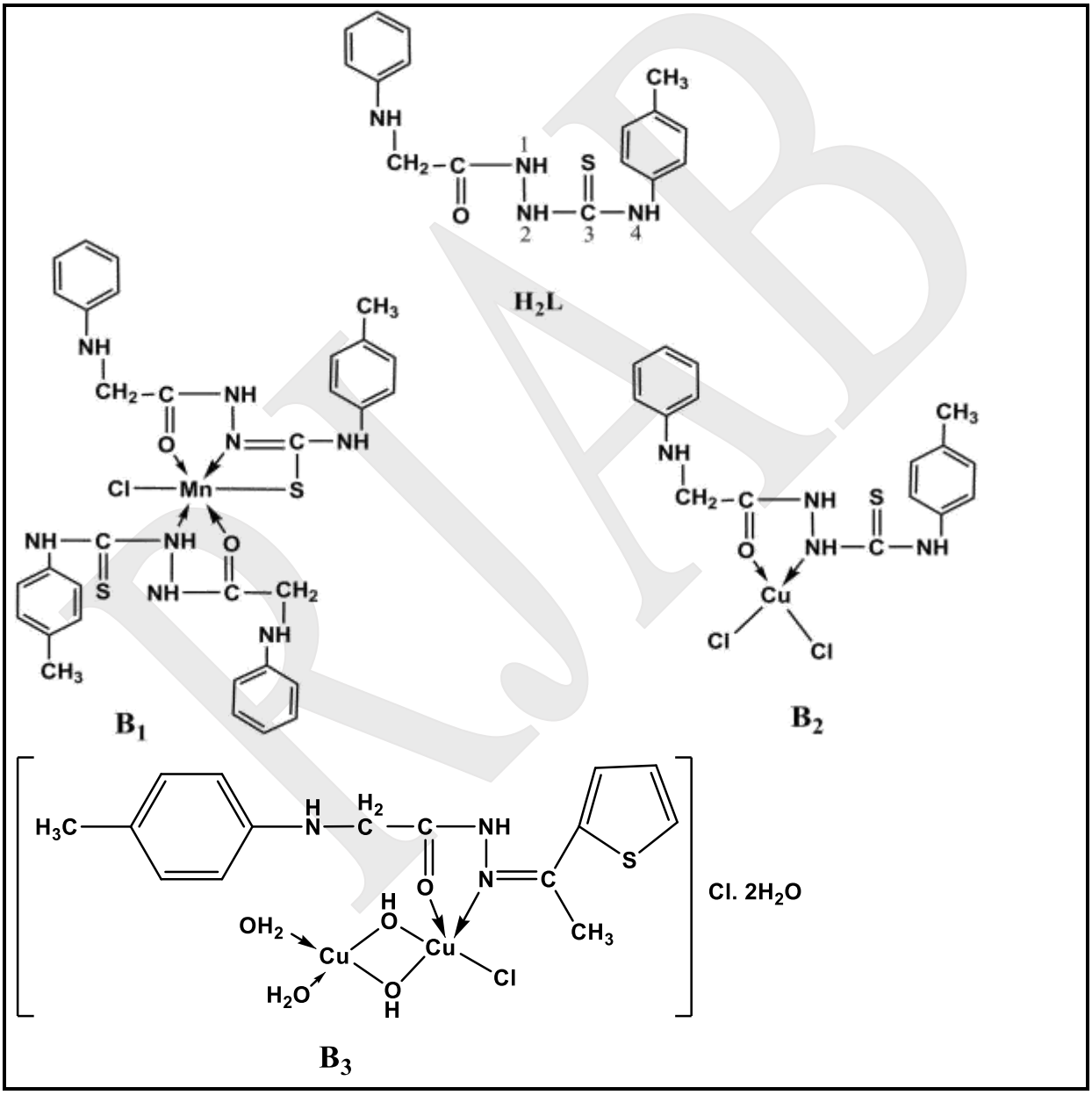

Scheme. 1. The suggested chemical structures of ligand and its complexes.

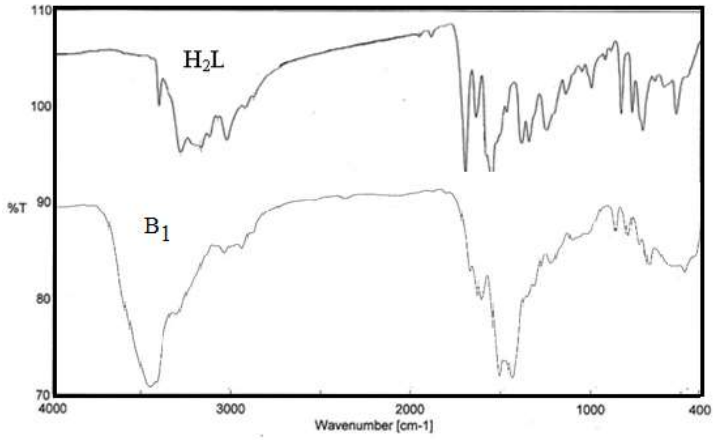

Fig. 1a : IR spectra of the ligand (H_2L) and Mn(II) complex (B_1)

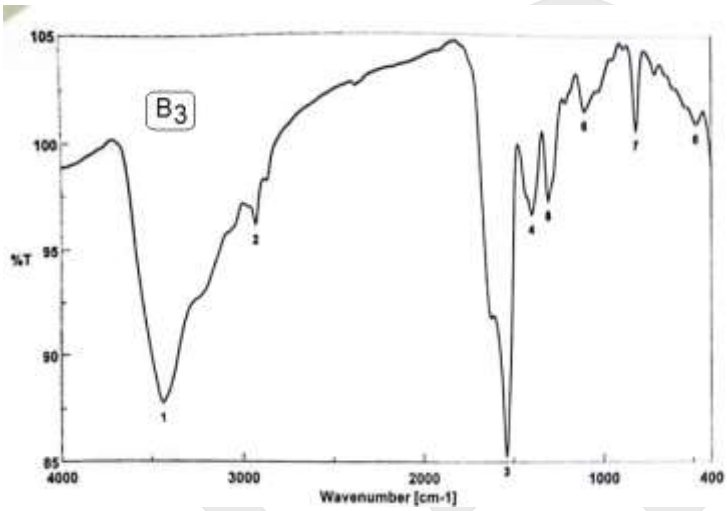

Fig. 1b. IR spectra of Cu(II) complex (B_3)

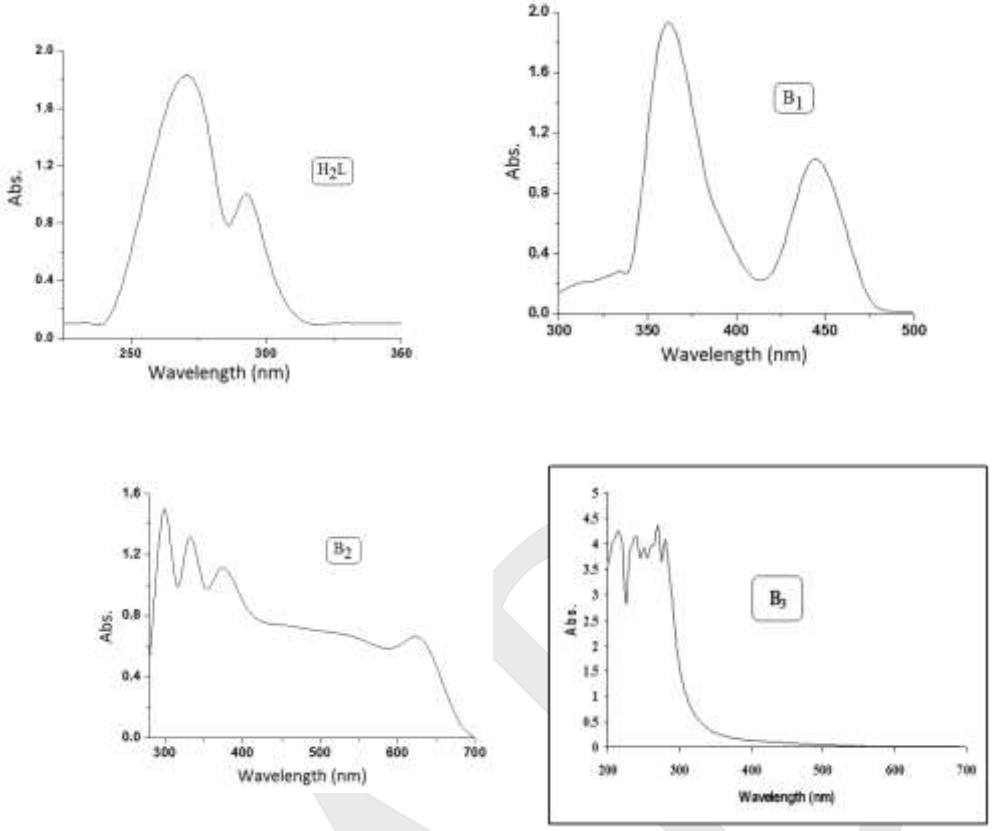

Fig.2 :Electronic spectra of the ligand (H_2L) and B_1 , B_2 and B3 complexes

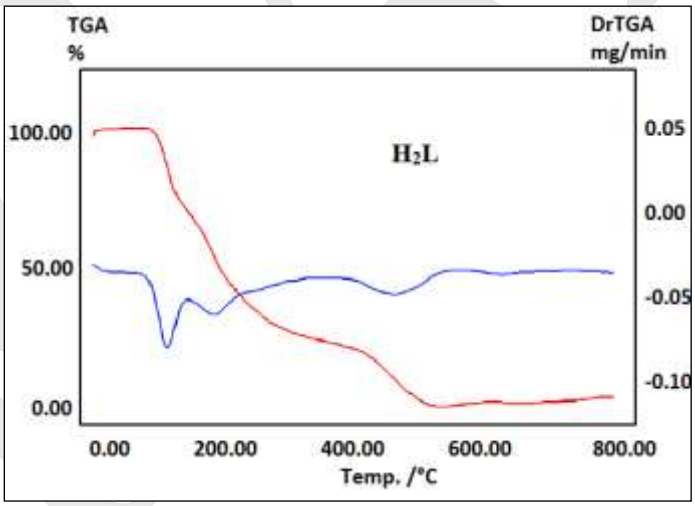

Fig.3. TGA / DTG curves of ligand (H_2L)

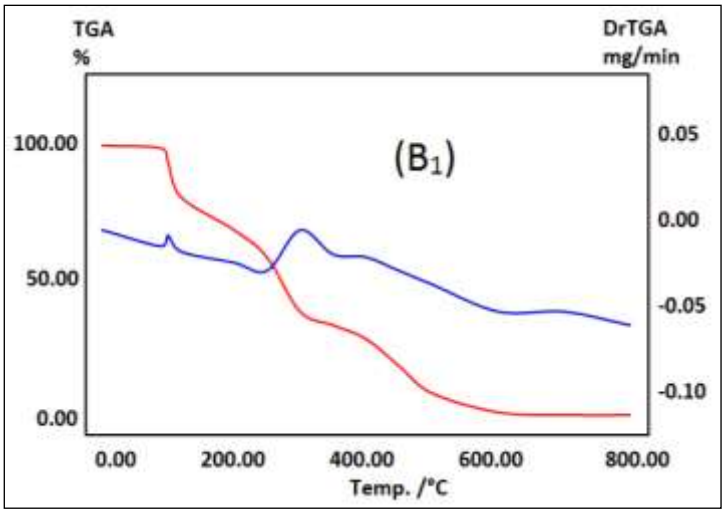

Fig.4. TGA / DTG curves of Mn(II) complex (B_1)

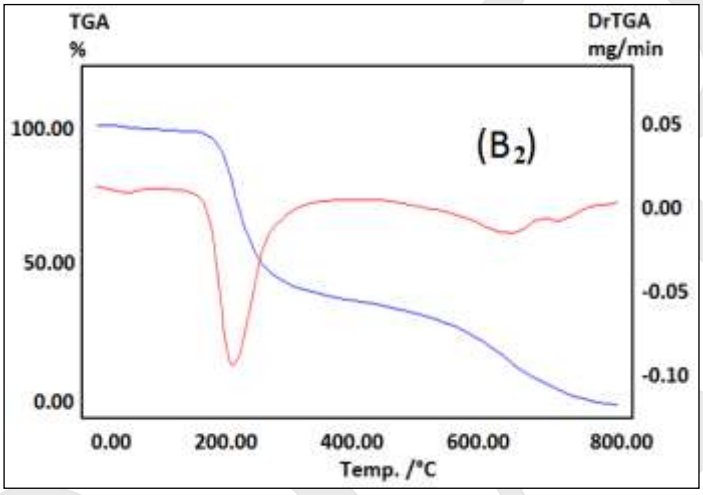

Fig. 5. TGA / DTG curves of Cu(II) complex (B_2)

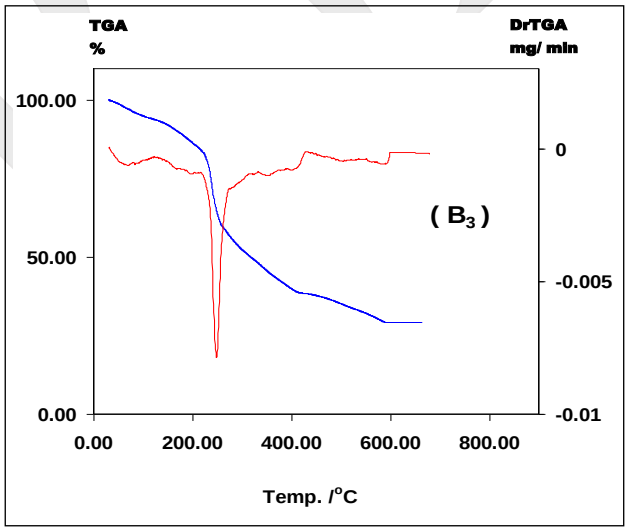

Fig. 6. TGA / DTG curves of Cu (II) complex (B3)

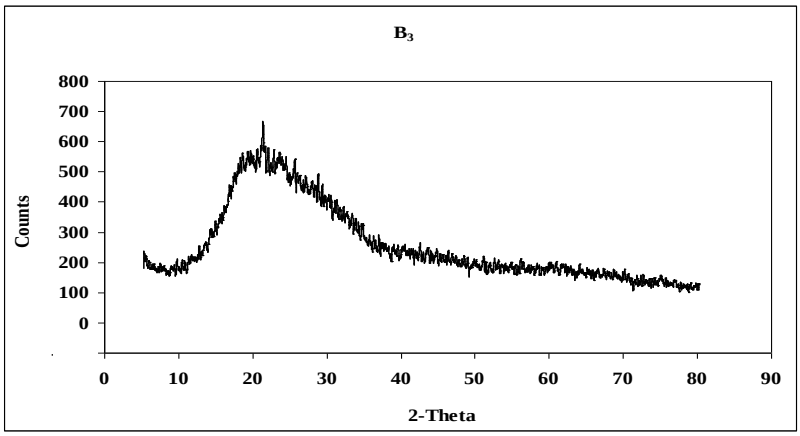

Fig.7. XRD Pattern of Cu (II) complex (B_3)

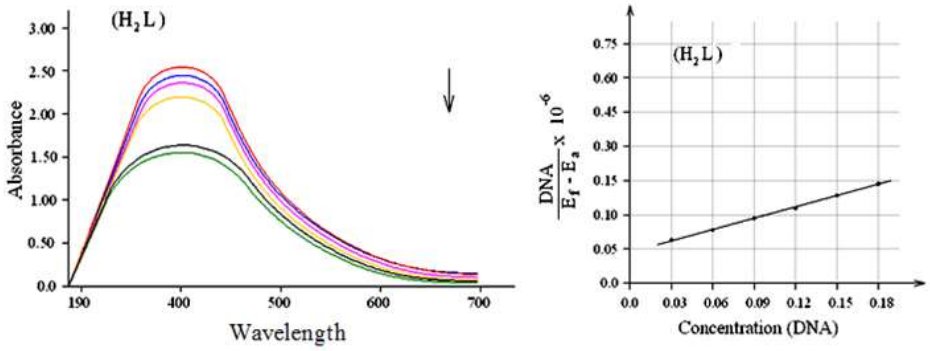

Fig. 8. Electronic absorption spectra of ligand (H2L) in the absence and presence of increasing amounts of CT-DNA. Arrows show the changes in absorbance with respect to an increase in the DNA concentration

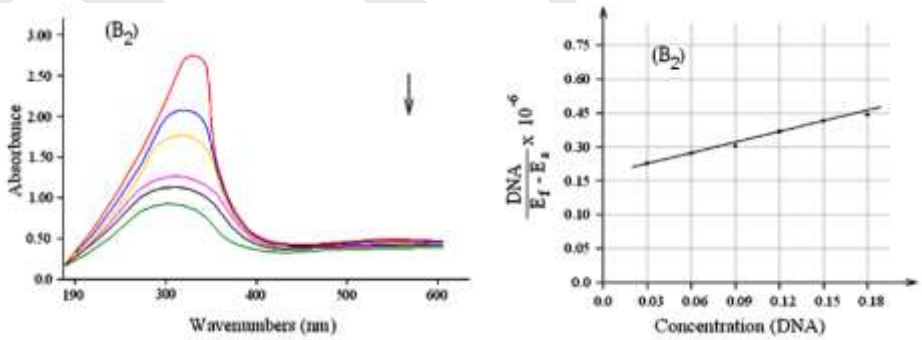

Fig.9. Electronic absorption spectra of cobalt complexes before and after irradiation (B_2) in the absence and presence of increasing amounts of CT-DNA. Arrows show the changes in absorbance with respect to an increase in the DNA concentration.

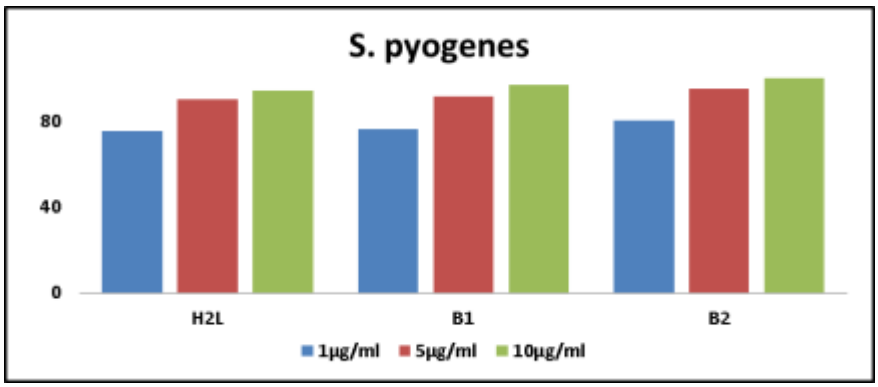

Fig. 10. In vitro antibacterial activity of ligand (H_2L) and Mn(II), Cu(II) complexes (B_1, B_2, B_3) against Gram positive bacteria (*Streptococcus pyogenes*)

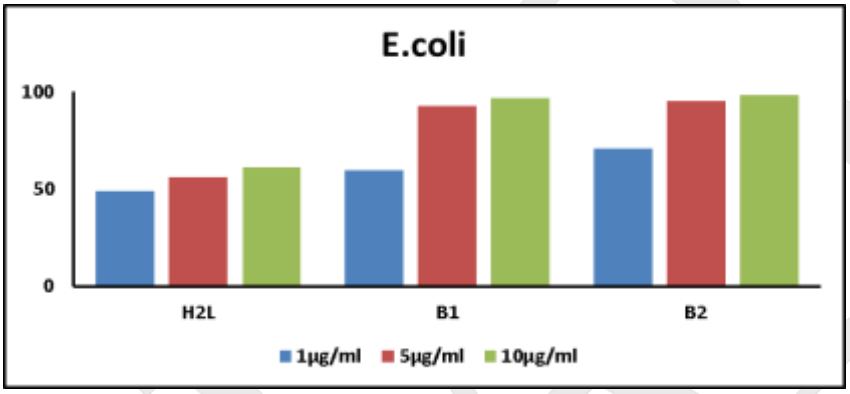

Fig. 11. In vitro antibacterial activity of ligand (H_2L) and Mn(II), Cu(II) complexes (B_1, B_2) against Gram negative bacteria (*Escherichia coli*).

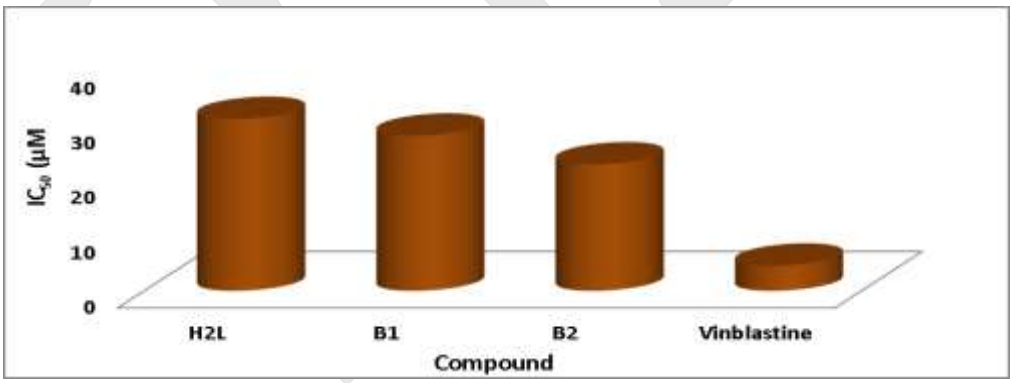

Fig.12. IC_{50} Values of Ligand (H_2L) and Mn (II), Cu (II) complexes (B_1, B_2) against Hep-G_2 carcinoma cell line compared to Vinblastine.